Submitted to

XXII International Symposium on Lepton-Photon Interactions at High Energy, June 30, 2005, Uppsala

Abstract: **401**

Sessions: **Flavor physics** and **QCD and hadron structure**

www-h1.desy.de/h1/www/publications/conf/conf_list.html

Acceptance corrected ratios of $D^*p(3100)$ and D^* yields and differential cross sections of $D^*p(3100)$ production H1

Collaboration

Abstract

The measurement of acceptance corrected ratios $\sigma(D^*p(3100))/\sigma(D^*)$ for electroproduction of the anti-charmed baryon state $D^*p(3100)$ decaying into D^* and p is presented. The analysis based on the 1996-2000 data is performed in the deep inelastic scattering region $1 < Q^2 < 100$ GeV^2, $0.05 < y_e < 0.7$.

1 Introduction

Motivated by recent experimental evidence for the production of a strange pentaquark Θ^+ in various reaction processes [1–3] the H1 experiment performed a search for a charmed pentaquark decaying to $D^{*-}p$ [1] in inelastic electron-proton collisions at centre-of-mass energies of 300 GeV and 320 GeV at HERA. A narrow resonance at a mass of 3099 MeV was observed in this decay channel [4]. Subsequent Θ_c searches by other high energy physics experiments did not confirm this observation [5–9].

It is difficult to draw conclusions from the apparently contradicting situation of observations and non-observations of pentaquarks in different high energy processes due to lack of understanding of its possible production mechanism. In order to facilitate further comparisons of experimental results and to investigate the production mechanism of the $D^*p(3100)$ resonance[2], its production phase space is explored in this paper. The data presented here include acceptance corrections based on a simple model assuming pentaquark production as part of the fragmentation process as suggested by the high energy pentaquark observations [3, 4]. Preliminary results on the acceptance corrected total yields ratio $R_{cor}(D^*p(3100)/D^*)$ in the visible D^*p and D^* range, differential distributions of the acceptance corrected cross section ratio $\sigma(D^*p(3100))/\sigma(D^*)$ as function of variables related to the event kinematics and the D^* meson and differential cross sections for $D^*p(3100)$ production are given.

2 Experimental Procedure

2.1 H1 Apparatus

The tracks from charged particles used in this analysis are reconstructed in the H1 central tracker, whose main components are two cylindrical drift chambers, the inner and outer central jet chambers (CJCs), covering the polar angle region $20^\circ < \theta < 160^\circ$. The H1 experiment uses a coordinate system in which the positive z-axis is defined by the direction of the outgoing proton beam. The polar angle θ of a particle is defined relative to this axis and is related to the pseudorapidity η by $\eta = -\ln\tan\theta/2$. The inner and outer CJCs are mounted concentrically around the beam-line, have 24 and 32 sense wires, respectively, and cover radii between 20 cm and 84 cm. The information from the CJC sense wires is digitized using 100 MHz FADCs, providing simultaneous charge and timing measurements. The CJCs lie within a homogeneous magnetic field of 1.15 T, which allows measurements of the transverse momenta of charged particles. Two additional drift chambers complement the CJCs by precisely measuring the z coordinates of track segments and hence assist in the determination of the particle's polar angle. The Central Silicon Tracker, consisting of two layers at radii of 6 cm and 10 cm, is also used to improve the charged particle track and event vertex reconstruction. The transverse momentum resolution of the central tracker is $\sigma(p_{\rm T})/p_{\rm T} \simeq 0.005\, p_{\rm T}$ [GeV] $\oplus\, 0.015$. The charge misidentification probability is negligible for particles originating from the primary vertex which have transverse momenta in the range relevant to this analysis.

[1]The charge conjugate state is always implied if not otherwise stated explicitly.

[2]Since the spin of the resonance is unknown the term $D^*p(3100)$ is used through out this paper although it is a candidate for the Θ_C.

The specific ionization energy loss of charged particles is derived from the mean of the inverse square-root of the charge collected by all CJC sense wires with a signal above threshold. The resolution is $\sigma(\mathrm{d}E/\mathrm{d}x)/(\mathrm{d}E/\mathrm{d}x) \simeq 8\%$ on average for minimum ionizing particles [10].

A lead/scintillating-fibre spaghetti calorimeter (SpaCal) is located in the direction of the outgoing electron beam. It contains both electromagnetic and hadronic sections and is used to detect the scattered electron in DIS events. The global properties of the hadronic final state are reconstructed using an algorithm which takes information from the central tracker, the SpaCal, and also from a Liquid Argon calorimeter, which surrounds the central tracker. The deep inelastic scattering (DIS) events studied in this paper are triggered on the basis of a scattered electron in the SpaCal, complemented by the signals in the CJCs and multi-wire proportional chambers in the central tracker. Further details of the H1 detector can be found in [11].

2.2 Event Sample

The analysis is carried out using data taken in the years 1996-2000, when HERA collided electrons[3] of energy 27.6 GeV with protons at 820 GeV (1996-1997) and 920 GeV (1998-2000). The integrated luminosity of the sample is $76\ \mathrm{pb}^{-1}$.

The scattered electron energy, measured in the SpaCal, is required to be above 8 GeV, and the virtuality of the exchanged photon[4] is required to lie in the range $1 < Q^2 < 100\ \mathrm{GeV}^2$, as reconstructed from the energy and polar angle of the electron. To ensure that the hadronic final state lies in the region well covered by the central trackers, the inelasticity of the event is required to satisfy $0.05 < y < 0.7$, calculated from the scattered electron kinemaitics. The z coordinate of the event vertex, reconstructed using the central tracker, is required to lie within 35 cm of the mean position for ep interactions. The difference between the total energy E and the longitudinal component of the total momentum p_z, calculated from the electron and the hadronic final state, is restricted to $35\ \mathrm{GeV} < E - p_z < 70\ \mathrm{GeV}$. This requirement suppresses photoproduction background, where a hadron fakes the electron signature.

2.3 Selection of D^* Meson and Proton Candidates

The selection of D^* mesons and proton candidates is the same as in [4] with further details given in [12]. Therefore only a brief summary is given here:

- The decay channel $D^* \to D^0\pi_s \to K\pi\pi_s$ is used to reconstruct D^* mesons.
- D^* candidates are required to have:
  - a minimum transverse momentum in the laboratory frame of $p_{\mathrm{T}}(D^*) > 1.5$ GeV,

[3]The analysis uses data from periods when the beam lepton was either a positron (88% of the total) or an electron (12% of the total).

[4]The inclusive DIS kinematic variables are defined as $Q^2 = -q^2$, $y = q \cdot p \,/\, k \cdot p$ and $x = -q^2 \,/\, 2q \cdot p$, where q, k and p are the 4-vectors of the exchanged photon, the incident electron and the incident proton, respectively.

- a pseudorapidity $\eta = -\log\tan(\Theta/2)$ in the laboratory frame in the range $-1.5 < \eta(D^*) < 1$ and
- a minimum inelasticity $z(D^*) = (E - p_z)_{D^*}/2yE_e$ of $z(D^*) > 0.2$, which account for the hard fragmentation of charmed hadrons.

In this kinematic region the combinatorial background to the D^* signal is small.

Some of the measured differential cross sections, namely the inelasticity distribution and the fragmentation function of the $D^*p(3100)$ baryon and the D^* meson from $D^*p(3100)$ decay, are strongly affected by the cut in $z(D^*)$. In order to obtain reasonable acceptances in the full variable range for these quantities the cut in $z(D^*)$ is replaced by a cut in the $D^*p(3100)$ fragmentation variable [5] $x_{obs}(D^*p)$ which is the momentum fraction of the charm quark carried by the $D^*p(3100)$ baryon by the following requirement

- $x_{obs}(D^*p) > min(0.5 \cdot p(p), 0.5)$, where $p(p)$ is the momentum of the proton. This selection cut allows to access the low x_{obs} and z regions with reasonable efficiency and gives the best sensitivity according to the pentaquark Monte Carlo and the non charm induced background as obtained from the data.

- D^* candidates having a mass difference $\Delta M_{D^*} = m(K\pi\pi_s) - m(K\pi)$ within ± 2.5 MeV of the nominal value $\Delta M_{D^*} = 145.4$ MeV are combined with oppositely charged proton candidates selected according to the proton likelihood based on the particles energy loss $\mathrm{d}E/\mathrm{d}x$ in the central trackers. The invariant mass distribution $M(D^*p) = m(K\pi\pi_s p) - m(K\pi\pi_s) + m(D^*)$ of these combinations is shown in figure 1 [4].

2.4 Monte Carlo Simulation

Monte Carlo simulation is used to determine acceptances for the D^* meson and for the $D^*p(3100)$ baryon. The acceptances were calculated using the RAPGAP 3.1 [13] event generator incorporating fragmentation according to the Lund string model [14] implemented in PYTHIA 6.1 [15].

For simulation of the $D^*p(3100)$ baryon it is assumed that pentaquarks are produced by fragmentation as suggested by the observation of the $D^*p(3100)$ resonance [4] in high energy ep scattering. The decay of the $D^*p(3100)$ was introduced by changing the properties of the $D_1(2420)$ and $D_2^*(2460)$ such that they decay to D^* meson plus proton with a natural width of zero, a mass of 3100 MeV and assuming isotropic decay. This model will be subsequently refered to as fragmentation production model.

The generated events are passed through the full detector simulation using GEANT 3.15 [16] and are subsequently subjected to the same reconstruction and analysis chain as the data.

[5] The measurement of the fragmentation function x_{obs} is studied in section 3.4.

3 Results

3.1 Total acceptance corrected $D^*p(3100)/D^*$ yields ratios

The observed yields ratio $R(D^*p(3100)/D^*) = (1.46{\pm}0.32)\%$ has been corrected for $D^*p(3100)$ and D^* acceptances with the approach described in the previous section. Because of our lack of knowledge about the $D^*p(3100)$ production mechanism and the ignorance of the angular momenta involved in its decay. The total acceptance corrected yields ratio is given for the visible range of the $D^*p(3100)$: $p_t(D^*p(3100)) > 1.5$ GeV, $-1.5 < \eta(D^*p(3100)) < 1.0$ and of the D^* meson: $p_t(D^*) > 1.5$ GeV, $-1.5 < \eta(D^*)$ <1.0, $z(D^*)$ >0.2. The same D^* visibility requirements are applied to the D^* meson originating from $D^*p(3100)$ baryon decay.

For this visible range the total acceptance corrected yields ratio is

$$R_{cor}(D^*p(3100)/D^*) = \left(1.59\ \pm\ 0.33(stat.)^{+\,0.33}_{-\,0.45}(syst.)\right)\ \%. \tag{1}$$

The systematic error includes the following sources of uncertainties:

- the dependence on the background shape used in the fit to the data shown in fig.1,
- the dependence on the D^* selection window in the ΔM_{D^*} distribution,
- the variation due to a cut of $z(D^*) > 0.1$,
- the effect of removing possible contributions from $D_1(2420)$ and $D_2^*(2460)$ due to pions misidentified as protons by requiring $|M(D^*\pi) - 2450\ \mathrm{MeV}|\ >\ 50$ MeV,
- uncertainties in the $\mathrm{d}E/\mathrm{d}x$ proton selection efficiency ,
- the effect of a softer fragmentation function of the $D^*p(3100)$ baryon,
- the variation of the $D^*p(3100)$ efficiency due to reweighting the $\eta(D^*p)$ distribution to better describe the observed distribution in fig.4a (see below).

The different contributions to the systematic error are summarized in table 1. The largest positive contribution to the systematic error on R_{cor} is obtained when the $D_1(2420)$ and $D_2^*(2460)$ veto cut is applied in the D^*p selection. The largest negative variation is observed when the cut against combinatorial background is reduced from $z(D^*) > 0.2$ to $z(D^*) > 0.1$.

The acceptance corrected ratio R_{cor} in the visible range (eq. 1) can be compared with the 95% C.L. upper limit of $R_{cor} < 0.51\%$ obtained by the ZEUS experiment in deep inelastic ep scattering [5] using a different definition of the visible range.

If acceptance corrections to the $D^*p(3100)$ signal are applied by extrapolating to the full D^* phase space from $D^*p(3100)$ decay based on the fragmentation production model a visible cross section ratio of

$$\sigma_{vis}(D^*p(3100))/\sigma_{vis}(D^*) = \left(2.48 \pm 0.52(stat.)^{+0.85}_{-0.64}(syst.)\right)\ \% \tag{2}$$

is obtained. The contribution to the systematic uncertainties on this ratio are given in table 2. Due to the extrapolation to the full D^* meson phase space in the $D^*p(3100)$ decay the largest positive variation of the ratio is observed when a softer fragmentation model has been used for the $D^*p(3100)$ baryon. Large negative variations are obtained when replacing the background suppression cut in the inelasticity z of the D^* meson by the cut in the fragmentation value of the $D^*p(3100)$ baryon, as described in section 2.3, or when using the shape of the background model in figure 1 for the fit of the D^*p mass distribution.

3.2 Differential distributions in $\sigma_{vis}(D^*p(3100))/\sigma_{vis}(D^*)$

In order to explore the properties of the events contributing to the $D^*p(3100)$ signal, acceptance corrected ratios $\sigma_{vis}(D^*p(3100))/\sigma_{vis}(D^*)$ have been determined from $M(D^*p)$ mass distributions in bins of a variety of phase space variables. In this section distributions related to event kinematics and to properties of the D^* mesons involved in the $D^*p(3100)$ decay are studied. For this preliminary analysis only statistical errors will be shown.

In figure 2 the acceptance corrected ratio $\sigma_{vis}(D^*p(3100))/\sigma_{vis}(D^*)$ is shown as a function of the hadronic mass W, the four momentum transfer squared of the virtual photon Q^2, and the invariant mass of the $c\bar{c}$ system, $\hat{s}_{obs}$. In leading order the invariant mass $\hat{s}_{obs}$ is given by

$$\hat{s}_{obs} = \frac{p_t^{*2}(c) + m_c^2}{z(c)(1 - z(c))}, \tag{3}$$

where $p_t^*(c)$ and $z(c)$ denote the transverse momentum in the photon-gluon system and the inelasticity of the charm quark, respectively. Since the quantities related to the charm quark are not accessible the invariant mass $\hat{s}_{obs}$ has to be reconstructed from the charmed hadrons instead. The expression 3 can be rewritten as

$$\hat{s}_{obs} = \frac{p_t^{*2}/x_{obs} + m_c^2 x_{obs}}{z(1 - z/x_{obs})}, \tag{4}$$

with the transverse momentum p_t^* in the centre-of-mass system, the fragmentation value x_{obs} and the inelasticity z of the $D^*p(3100)$ and D^*, respectively.

Figure 2 also includes the expectation for $\sigma_{vis}(D^*p(3100))/\sigma_{vis}(D^*)$ using the fragmentation production model. Since the absolute normalization of the $D^*p(3100)$ rate is not fixed in the model, the $D^*p(3100)$ yield is normalized such to reproduce the ratio R_{cor} in (1). The expected variation of the ratio with W and $\hat{s}_{obs}$ is a consequence of threshold effects due to the significantly different masses of the $D^*p(3100)$ and D^*. The observed dependence on W and on Q^2 is well described by this model, while it is significantly above the data at large $\hat{s}_{obs}$.

In order to investigate the properties of the D^* mesons contributing to the $D^*p(3100)$ resonance the ratio $\sigma_{vis}(D^*p(3100))/\sigma_{vis}(D^*)$ is shown in figure 3 as a function of the pseudorapidity $\eta(D^*)$ and the transverse momentum $p_t(D^*)$, both in the laboratory frame, the inelasticity $z(D^*)$ and the pseudorapidity $\eta^*(D^*)$ in the hadronic centre-of-mass system. Also shown are the expectations from the model.

The most striking feature in the data is the suppression of the $D^*p(3100)$ baryon relative to D^* meson production in the near to central region both in the laboratory frame and in the hadronic centre-of-mass system. Such a dependence is not predicted by the fragmentation production model. The data indicate that $D^*p(3100)$ baryon production is closer to the photon direction than normal D^* meson production. Figure 3 also shows the ratio $\sigma_{vis}(D^*p(3100))/\sigma_{vis}(D^*)$ as a function of the inelasticity $z(D^*)$. The $D^*p(3100)$ baryons contribute mainly at small $z(D^*)$ as expected from the masses of the particles involved in the $D^*p(3100)$ decay[6] within the framework of the fragmentation production model.

3.3 Differential $D^*p(3100)$ cross sections

To get information of the $D^*p(3100)$ production mechanism $D^*p(3100)$ differential cross sections in $D^*p(3100)$ quantities are presented in this section. The fragmentation production model is used for acceptance corrections. As in the previous section only statistical errors are given in the figures.

In figure 4 the differential $D^*p(3100)$ production cross section is shown as a function of the pseudorapidity $\eta(D^*p)$ and the transverse momentum $p_t(D^*p)$, both in the laboratory frame, the inelasticity $z(D^*p)$ and the pseudorapidity $\eta^*(D^*p)$ in the hadronic centre-of-mass system. The $D^*p(3100)$ production cross section shows the same features as a function of the pseudorapidities $\eta(D^*p)$ and $\eta^*(D^*p)$ than observed for the ratio $\sigma_{vis}(D^*p(3100))/\sigma_{vis}(D^*)$ as a function of the D^* variables. Within the quite large statistical errors the shapes of the $z(D^*p)$ and of the $p_t(D^*p)$ distributions are consistent with the fragmentation production model. These two distributions are suggesting that boson gluon fusion is the source for the production of $D^*p(3100)$ baryons while the pseudorapidity distributions are not evidently supporting this picture.

3.4 Fragmentation function

For the comparison of the observation of the $D^*p(3100)$ resonance in deep inelastic ep scattering by H1 with results obtained in other high energy physics processes the momentum fraction from the parent charm quark carried by the $D^*p(3100)$ and the D^* from $D^*p(3100)$ decay is of specific interest.

In order to measure the $D^*p(3100)$ fragmentation function and the D^* hadronization function for D^* mesons from $D^*p(3100)$ decay the analysis is performed in the hadronic centre-of-mass system. The method used to reconstruct the fragmentation variable x_{obs} is sketched in figure 5. It is similar to the method presented in reference [17]. In the plane perpendicular to the photon direction in this frame the charm quarks from the leading order boson gluon fusion process exhibit a back-to-back signature similar to the situation in e^+e^- annihilation. In this way it becomes possible to reconstruct the visible quark energy even close to threshold from the hadronic final state. For the analysis only those particles with $\eta^* > 0$ are used which belong to the photon hemisphere (fig. 5a). Those particles which have angle smaller than $\pi/2$ with respect to the D^* direction in the projection plane perpendicular to the photon direction are

[6] In order to access the small $z(D^*)$ region the cut in this variable is replaced by a minimum requirement in the $D^*p(3100)$ fragmentation variable given in section 2.3.

subsequently assigned to the D^* hemisphere. The $D^*p(3100)$ fragmentation variable and the D^* hadronization variable can then be defined as

$$x_{obs} = \frac{(E - p_z)}{\sum\limits_{h \in hemi} (E - p_z)_h}, \tag{5}$$

where $(E - p_z)$ denotes the value of $E - p_z$ of the hadrons in the laboratory frame. In the enumerator enter the quantities of the $D^*p(3100)$ baryon or the D^* meson, respectively, while the sum in the denominator runs over all hadrons attributed to the D^* hemisphere in the plane perpendicular to the photon direction. This method yields a definition of the fragmentation function similar to what is used in e^+e^- annihilation.

In figure 6 the acceptance corrected cross section ratio $\sigma_{vis}(D^*p(3100))/\sigma_{vis}(D^*)$ as a function of the D^* hadronization value $x_{obs}(D^*)$ and the differential $D^*p(3100)$ cross section as a function of $x_{obs}(D^*p)$ are shown together with the prediction from the model. The ratio $\sigma_{vis}(D^*p(3100))/\sigma_{vis}(D^*)$ increases with decreasing $x_{obs}(D^*)$ value which means that D^* mesons originating from $D^*p(3100)$ decay are significantly softer than inclusive D^* mesons which carry most of the charm quark energy. In case of inclusive measurements of D^* meson production in deep inelastic scattering at HERA the most probable fragmentation value is $x_{obs}(D^*) \approx 0.7$ [17]. The significantly softer $x_{obs}(D^*)$ distribution of D^* mesons contributing to the $D^*p(3100)$ resonance is consistent with the expectation from the decay of the $D^*p(3100)$ particle.

In figure 6b the differential cross section $d\sigma_{vis}(D^*p(3100))/dx_{obs}(D^*p)$ is shown as a function of $x_{obs}(D^*p)$. The $D^*p(3100)$ fragmentation function is very hard compared to the D^* hadronization function of figure 6a. A hard fragmentation is expected for charmed hadrons. Within the limited statistics this differential cross section indicates a harder fragmentation function for the $D^*p(3100)$ baryon compared to that observed in inclusive D^* mesons production [17], which is expected due to the larger $D^*p(3100)$ mass compared to the D^* mass.

4 Conclusions

A detailed analysis of the exotic $D^*p(3100)$ baryon has been presented. An acceptance corrected yields ratio $R_{cor}(D^*p(3100)/D^*) = \big(1.59 \pm 0.33(stat.)^{+\,0.33}_{-\,0.45}(syst.)\big)$ % for the visible $D^*p(3100)$ and D^* range has been observed. In the case of the $D^*p(3100)$ the visibility requirement is simultaneously imposed to the $D^*p(3100)$ as well as to its decay product, the D^* meson. When extrapolating to the full phase space of the decay products one observes a ratio of the visible cross sections of $\sigma_{vis}\left(D^*p(3100)\right)/\sigma_{vis}(D^*) = \big(2.48 \pm 0.52(stat.)^{+0.85}_{-0.64}(syst.)\big)$ %.

Differential distributions of $\sigma_{vis}(D^*p(3100))/\sigma_{vis}(D^*)$ as a function of event kinematics and D^* quantities have been presented. In general the fragmentation production model leads to a reasonable description of the distributions with some exceptions. The most striking deviation from the expectation is observed in $\eta(D^*)$ and $\eta^*(D^*)$. Compared to inclusive D^* production the $D^*p(3100)$ production seems to be suppressed in the close to central rapidity regions in both frames. The differential $D^*p(3100)$ cross sections as a function of $D^*p(3100)$ variables show the same effect. The $D^*p(3100)$ fragmentation function is hard, consistent with the expectation for a charmed hadron with the given mass. The hadronization function for D^* mesons contributing to the $D^*p(3100)$ resonance is much softer than observed in inclusive D^* mesons production. This observation is consistent with the expectation for a particle with a mass of 3100 MeV decaying to D^* meson plus proton.

References

[1] T. Nakano *et al.*, (LEPS), Phys. Rev. Lett. **91** (2003) 012002;
S. Stepanyan *et al.*, (CLAS), Phys. Atom. Nuclei **66** (2003) 1715;
J. Barth *et al.*, (SAPHIR), Phys. Lett. B **572** (2003) 127;
V. Kubarovsky *et al.*, (CLAS), Phys. Rev. Lett. **92** (2004) 03201 [erratum-ibid. 92 (2004) 049902].

[2] V. V. Barnim *et al.*, (DIANA), Phys. Atom. Nucl. **66** (2003) 1715 [Yad. Fiz. 66 (2003) 1763];
A. E. Asratyan, A. G. Dolgolenko and M. A. Kubantsev, Phys. Atom. Nucl. **67** (2004) 682;
A. Aleev *et al.*, (SVD), hep-ex/0401024;
A. Airapetian *et al.*, (HERMES), Phys. Lett. B **585** (2004) 127;
M. Abdel-Bary *et al.*, (COSY-TOF),Phys. Lett. B **595** (2004) 127.

[3] S. Chekanov *et al.* [ZEUS Collaboration], Phys. Lett. **591** (2004) 7.

[4] A.Aktas *et al.* [H1 Collaboration] Phys. Lett **B 588** (2004) 17.

[5] S. Chekanov *et al.* [ZEUS Collaboration], Eur. Phys. J. **C 38** (2004) 29.

[6] S. R. Armstrong, hep-ex/0410080; S. Schael *et al.*, (ALPEH), Phys. Lett. B **599**(2004) 1.

[7] D. O. Litvintsev, (CDF), hep-ex/0410024.

[8] K. Stenson (FOCUS), hep-ex/0412021.

[9] R. Mizuk *et al.*, (Belle), hep-ex/0411005.

[10] J. Steinhart, 'Die Messung des totalen $c\bar{c}$-Photoproduktions-Wirkungsquerschnittes durch die Rekonstruktion von Λ_c Baryonen unter Verwendung der verbesserten $\mathrm{d}E/\mathrm{d}x$ Teilchenidentifikation am H1 Experiment bei HERA', Ph.D. thesis, 1999, Universität Hamburg (in German, available from
`http://www-h1.desy.de/publications/theses_list.html`).

[11] I. Abt *et al.* [H1 Collaboration], Nucl. Inst. Meth. **A386** (1997) 310;
I. Abt *et al.* [H1 Collaboration], Nucl. Inst. Meth. **A386** (1997) 348.

[12] S. Aid *et al.* [H1 Collaboration], Nucl. Phys. **B472** (1996) 32 [hep-ex/9604005];
C. Adloff *et al.* [H1 Collaboration], Nucl. Phys. **B545** (1999) 21 [hep-ex/9812023];
C. Adloff *et al.* [H1 Collaboration], Phys. Lett. **B528** (2002) 199 [hep-ex/0108039].

[13] H. Jung, Comp. Phys. Comm. **71** (1992) 15.

[14] B. Andersson, G. Gustafson, G. Ingelman and T. Sjöstrand, Phys. Rept. **97** (1983) 31.

[15] T. Sjöstrand *et al.*, Comp. Phys. Commun. **135** (2001) 238 [hep-ph/0010017].

[16] R. Brun *et al.*, GEANT3, Technical Report CERN-DD/EE/84-1, CERN, 1987.

[17] H1 Collaboration, contributed paper to the Lepton-Photon Conference 2005, Abstract # 407, Uppsala, Sweden.

Variation	$\frac{\Delta R_{cor}}{R_{cor}}$ [%]
Background shape determined from background model in Fig. 1	-12
$\Delta M(D^*)$ window reduced to 1.5 MeV	-9
Visible D^* region extended down to $z(D^*)$ >0.1	-21
Require $\|M(D^*\pi) - 2450\ \mathrm{MeV}\| > 50$ MeV for the D^*p combinations	+18
dE/dx calibration	$\pm$10
Soft fragmentation of $D^*p(3100)$	-5
Reweighting of $\eta(D^*p(3100))$	-3
Total	-28 + 21

Table 1: Relative systematic errors on the acceptance corrected yields ratio R_{cor} for the visible $D*$ meson region.

Variation	$\frac{\Delta \frac{\sigma_{vis}(D^*p(3100))}{\sigma_{vis}(D^*)}}{\frac{\sigma_{vis}(D^*p(3100))}{\sigma_{vis}(D^*)}}$ [%]
Background shape determined from background model in Fig. 1	-14
$\Delta M(D^*)$ window reduced to 1.5 MeV	-10
Visible D^* region extended down to $z(D^*)$ >0.1	-8
$z(D^*)$ replaced by cut in the $D^*p(3100)$ fragmentation variable x_{obs}	-15
Require $\|M(D^*\pi) - 2450\ \mathrm{MeV}\| > 50$ MeV for the D^*p combinations	+17
dE/dx calibration	$\pm$10
Soft fragmentation of $D^*p(3100)$	+28
Reweighting of $\eta(D^*p(3100))$	-4
Total	-26 + 34

Table 2: Relative systematic errors on the acceptance corrected visible cross section ratio $\sigma_{vis}(D^*p(3100))/\sigma_{vis}(D^*)$.

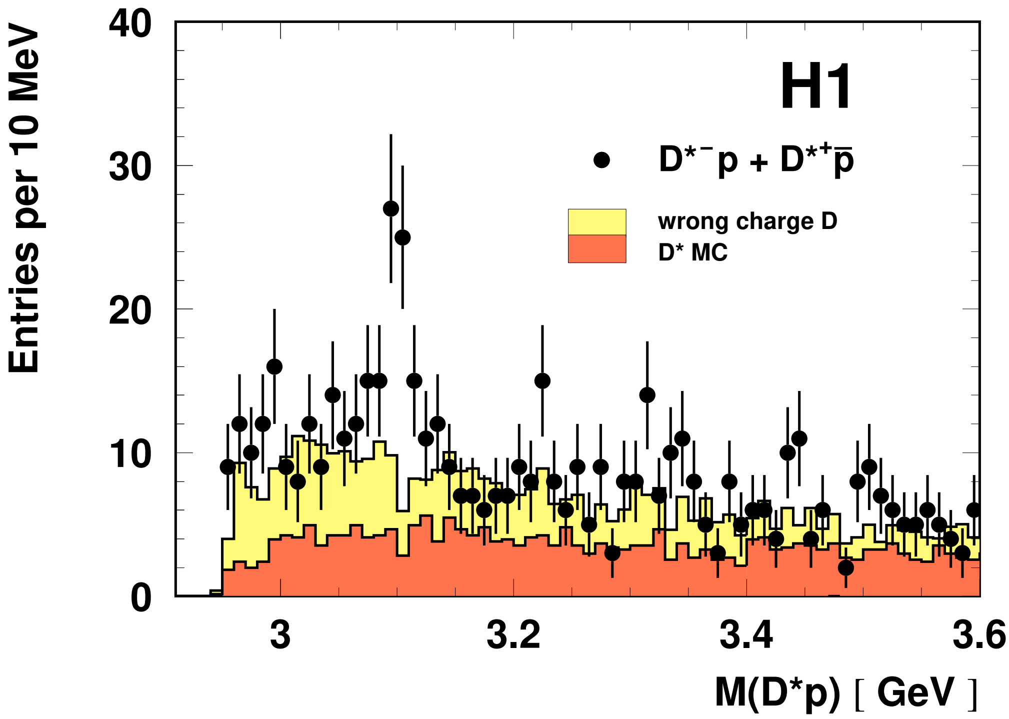

Figure 1: Distributions in $M(D^*p)$ for opposite-charge D^*p combinations. The data are compared with a two-component background model in which “wrong charge D” $K^\pm\pi^\pm$ combinations are used to describe non-charm related background and the “D^* MC” simulation describes background involving real D^* mesons (from ref [4]).

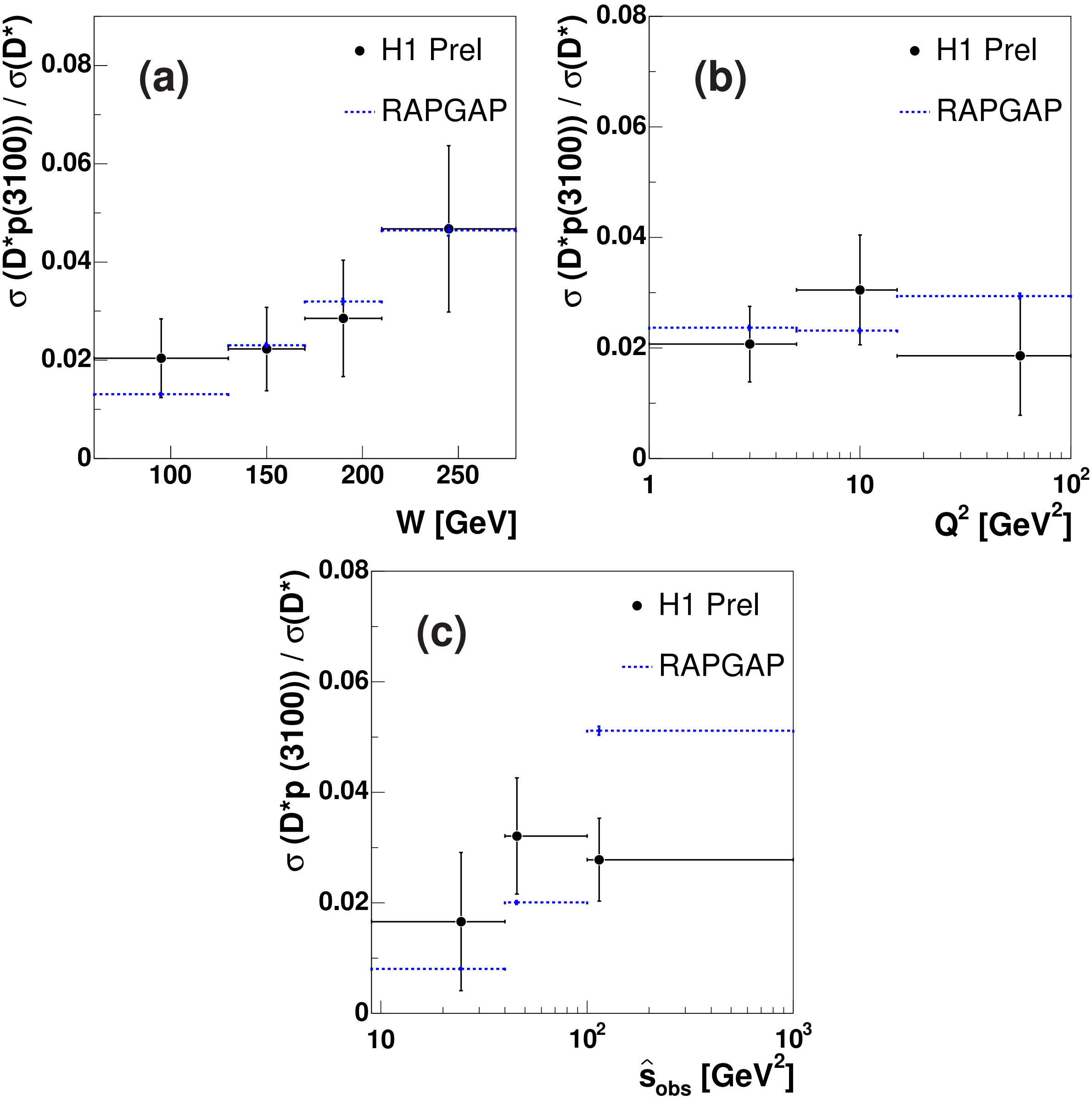

Figure 2: Acceptance corrected ratios $\sigma_{vis}(D^*p(3100))/\sigma_{vis}(D^*)$ as a function of the kinematic variables (a) W, (b) Q^2 and (c) $\hat{s}_{obs}$. Data (closed symbols) are compared with the expectation (dashed line) of RAPGAP 3.1 which assumes the same mechanism for D^* and $D^*p(3100)$ production. Only statistical errors are shown.

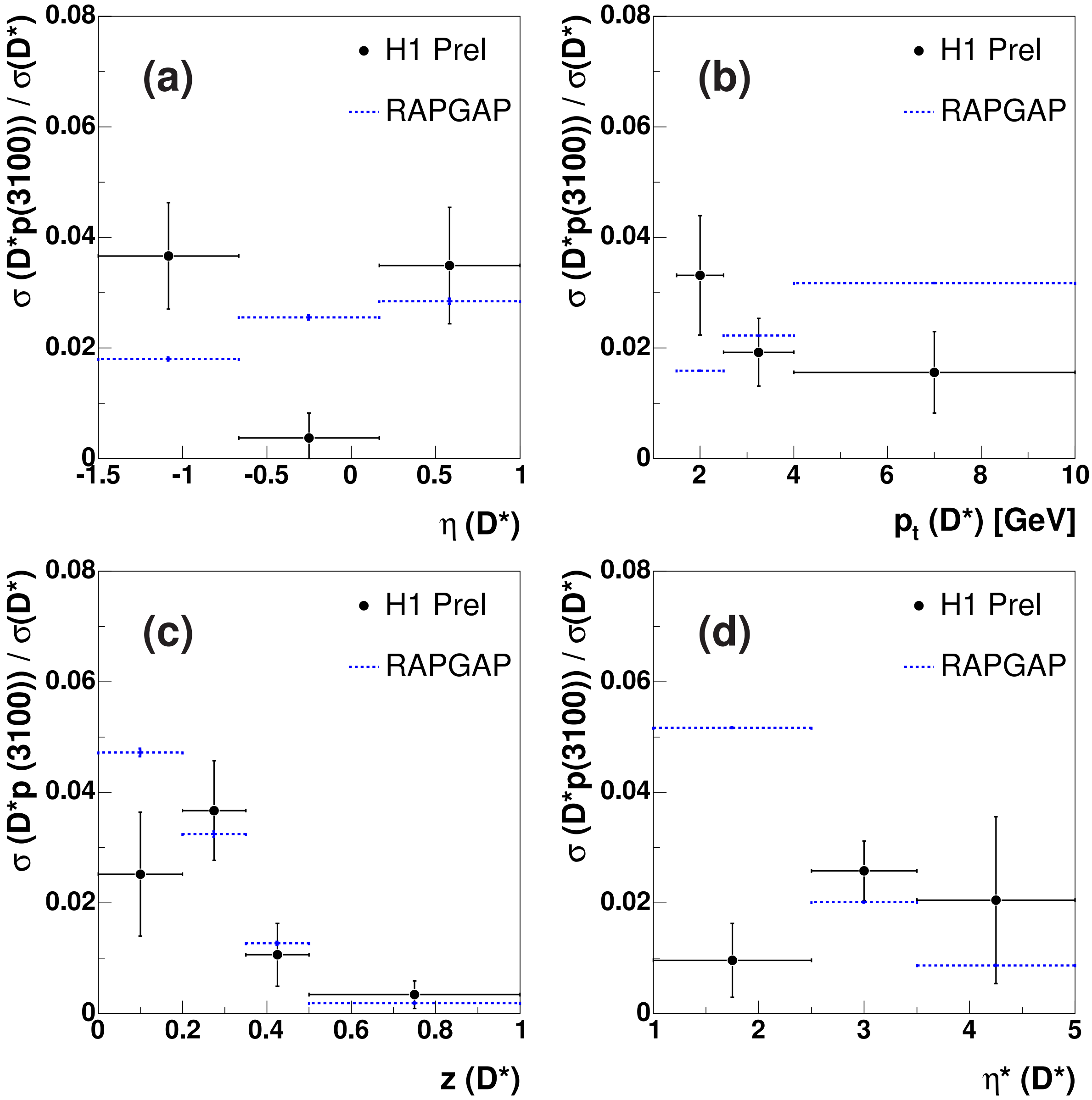

Figure 3: Acceptance corrected ratios $\sigma_{vis}(D^*p(3100))/\sigma_{vis}(D^*)$ as a function of D^* variables (a) $\eta(D^*)$ and (b) $p_t(D^*)$ both in the laboratory frame, (c) $z(D^*)$ and (d) $\eta^*(D^*)$ in the hadronic centre-of-mass system. Data (closed symbols) are compared with the expectation (dashed line) of RAPGAP 3.1 which assumes the same mechanism for D^* and $D^*p(3100)$ production. Only statistical errors are shown.

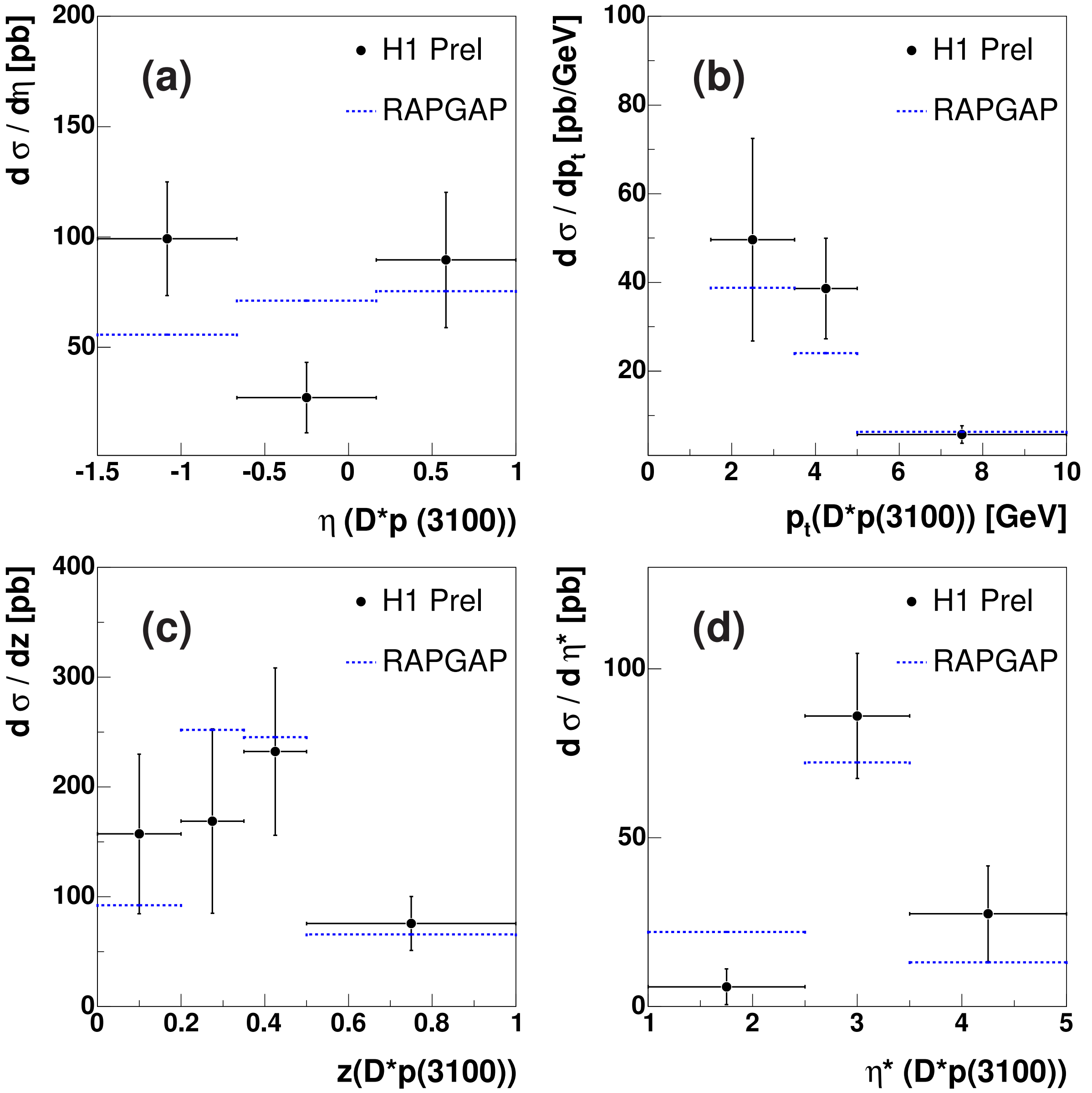

Figure 4: Differential $(D^*p(3100))$ cross sections as a function of D^*p variables (a) $\eta(D^*p)$ and (b) $p_t(D^*p)$ both in the laboratory frame, (c) $z(D^*p)$ and (d) $\eta^*(D^*p)$ in the hadronic centre-of-mass system. Data (closed symbols) are compared with the expectation (dashed line) of RAPGAP 3.1 which assumes the same mechanism for D^* and $D^*p(3100)$ production. Only statistical errors are shown.

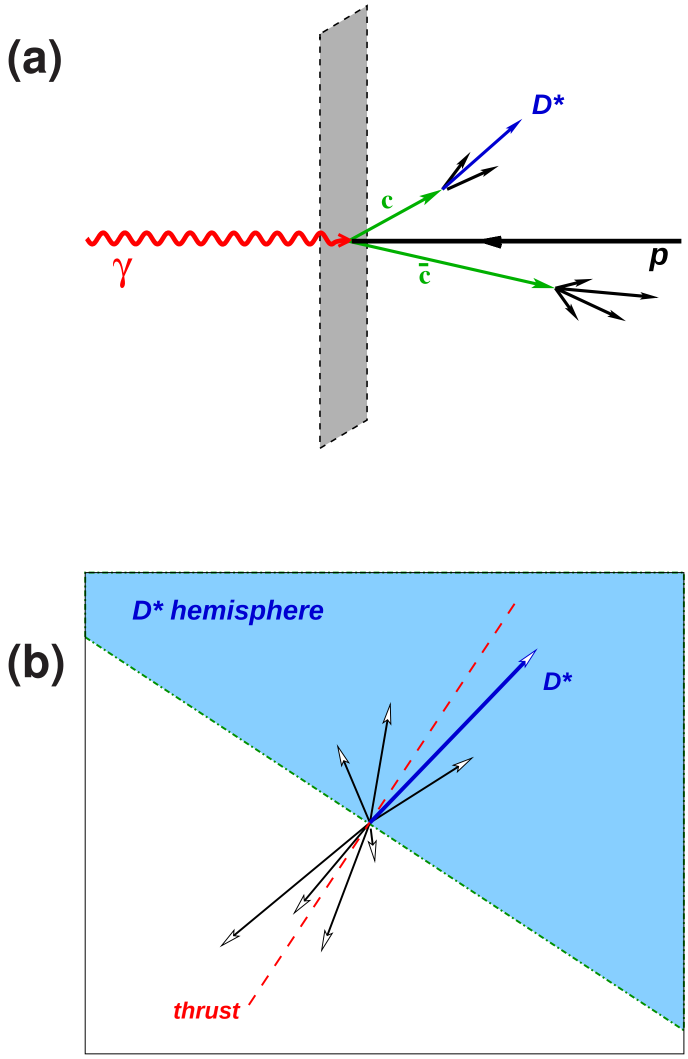

Figure 5: Sketch of the method to reconstruct the visible charm quark energies in ep scattering close to threshold. (a) The hadrons in the photon hemisphere of the hadronic centre-of-mass system are projected to the plane perpendicular to the photon direction. (b) The hadrons in the $D*$ hemisphere are used to reconstruct the visible charm quark energy.

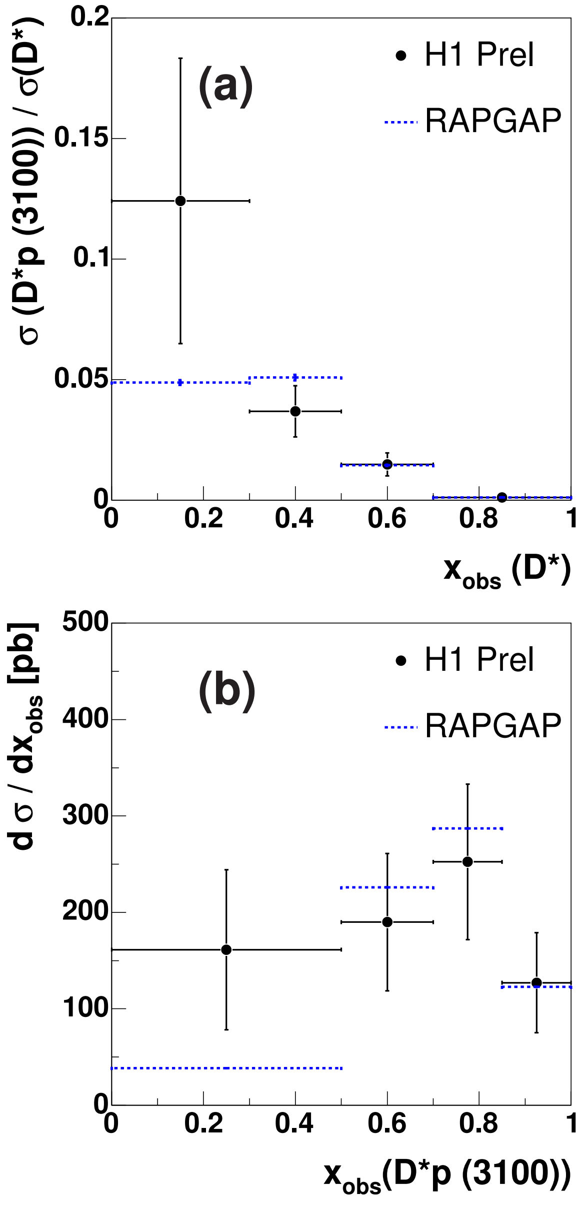

Figure 6: Acceptance corrected ratio $\sigma_{vis}(D^*p(3100))/\sigma_{vis}(D^*)$ as a function of the D^* hadronization fraction $x_{obs}(D^*)$ in (a) and differential cross section $d\sigma_{vis}(D^*p(3100))/dx_{obs}(D^*p)$ in (b). Data (closed symbols) are compared with the expectation (dashed line) of RAPGAP 3.1 which assumes the same mechanism for D^* and $D^*p(3100)$ production. Only statistical errors are shown.